SUPPLEMENTARY INFORMATION

1-D nanostructure comprising porous Fe_2O_3/Se composite nanorods with numerous nanovoids, and their electrochemical properties for use in lithium-ion batteries

Jung Sang Cho[ab], Jin-Sung Park[a], Kyung Min Jeon[a], and Yun Chan Kang[a]*

[a]Department of Materials Science and Engineering, Korea University, Anam-dong, Seongbuk-gu, Seoul 136-713, Republic of Korea

[b]Department of Engineering Chemistry, Chungbuk National University, Chungbuk 361-763, Republic of Korea

E-mail: yckang@korea.ac.kr Fax: +82-2-928-3584; Tel: +82-2-3290-3268

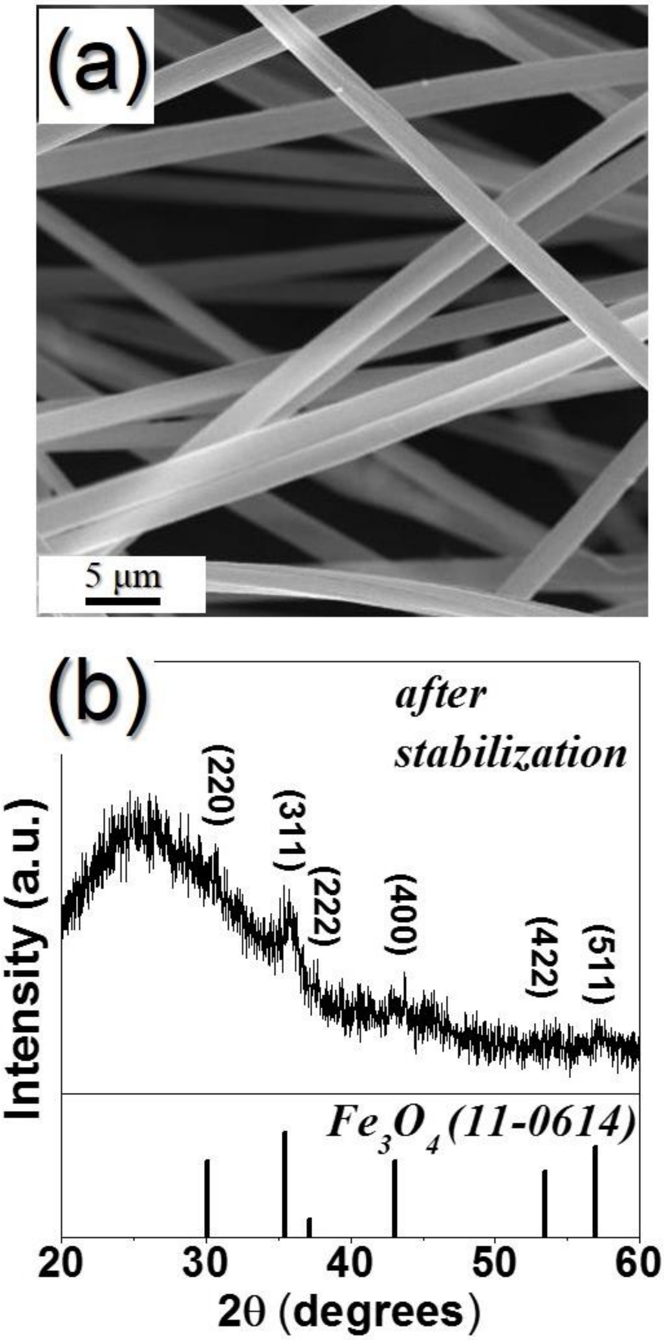

Fig. S1. (a) SEM image and (b) XRD pattern of the Fe_3O_4-carbon composite nanofibers after strabilization at 120 ^{o}C in air.

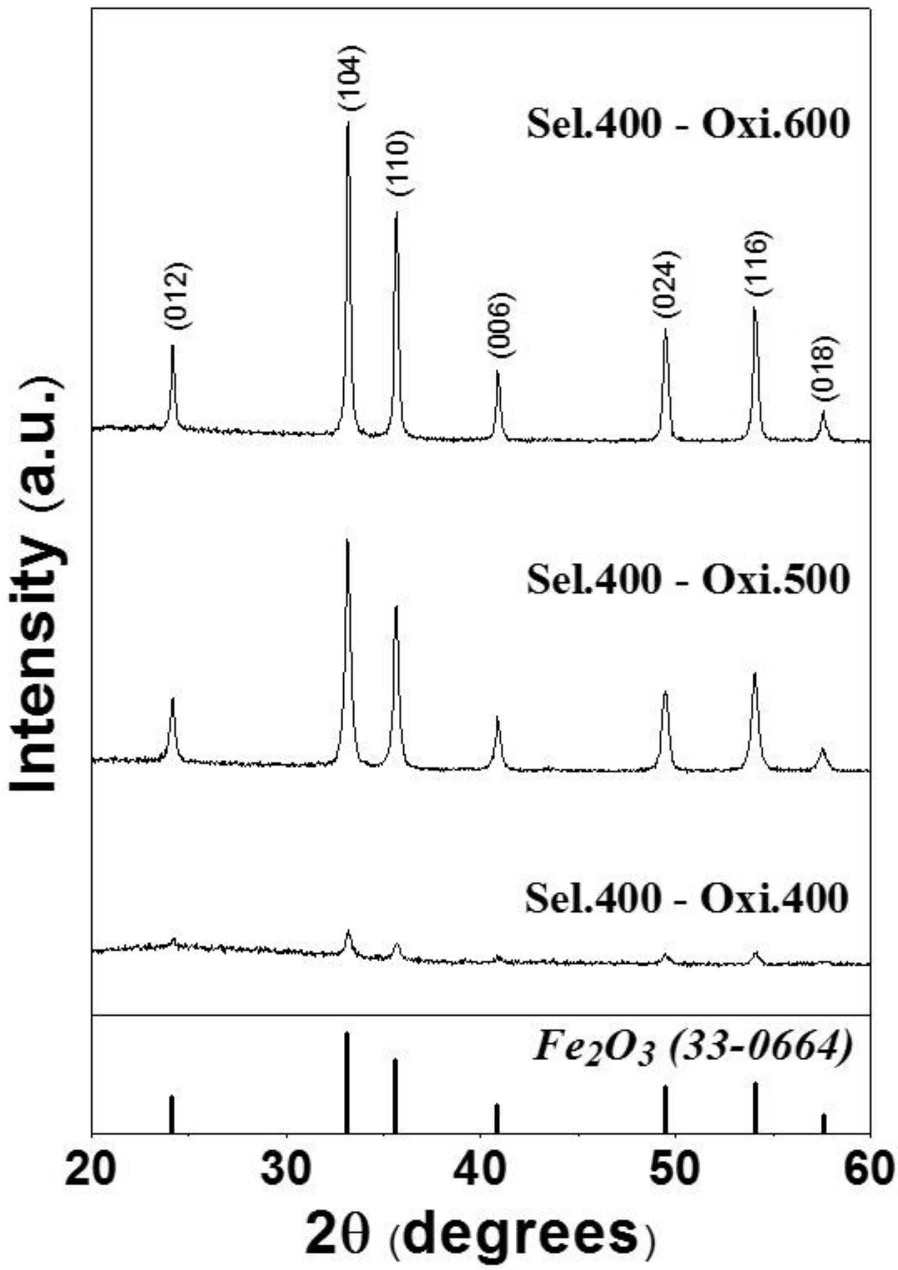

Fig. S2. XRD patterns of the 1-D nanostructures comprising nanorods obtained after selenization at 400 °C and subsequent oxidation at 400, 500, and 600°C.

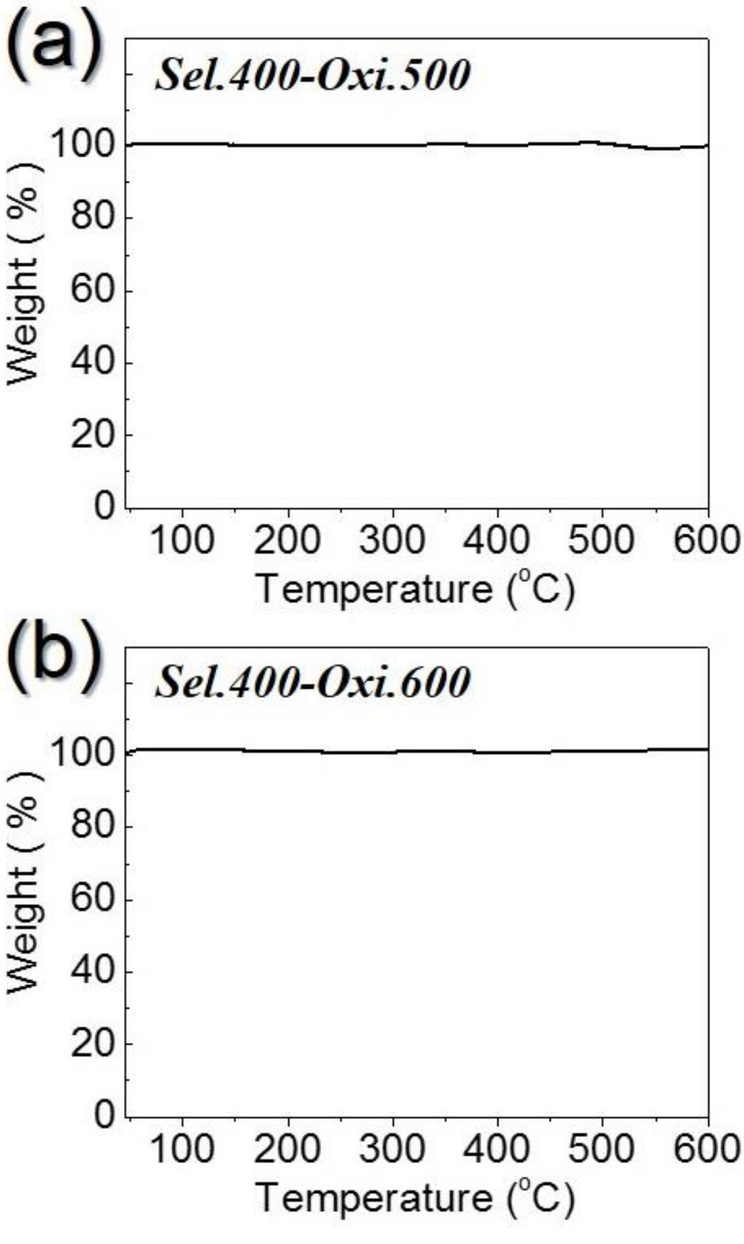

Fig. S3. TG analysis of the 1-D nanostructures comprising nanorods obtained after selenization at 400 °C and subsequent oxidation at 500 and 600°C: (a) Sel.400-Oxi.500, and (b) Sel.400-Oxi.600.

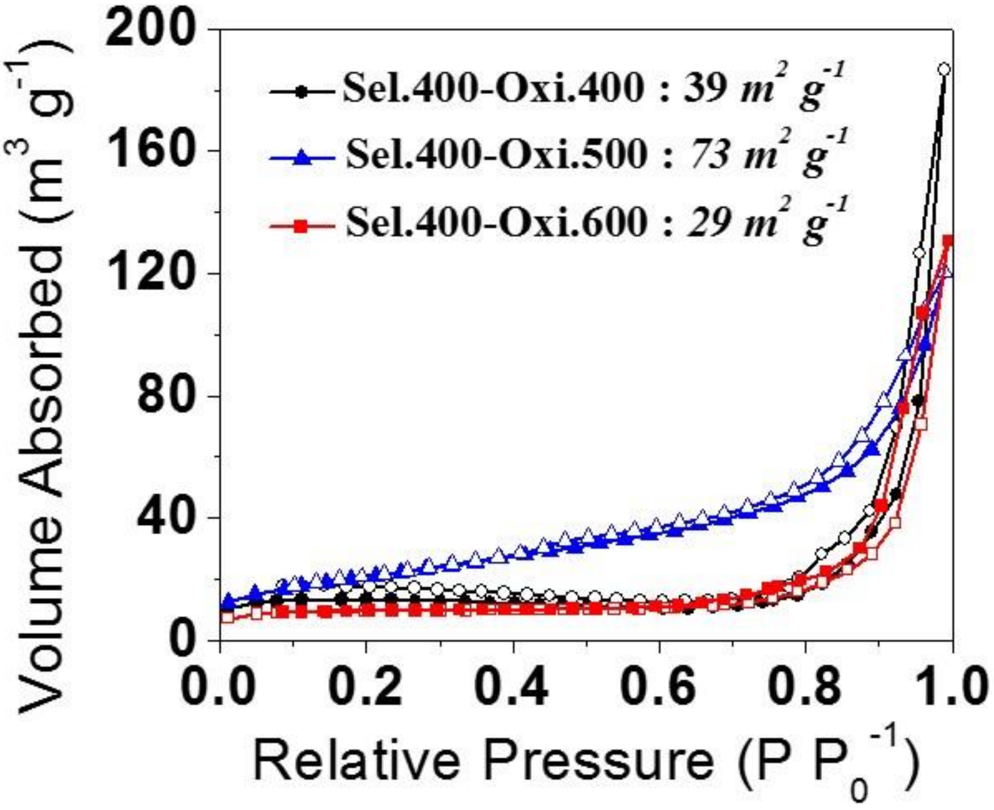

Fig. S4. N_2 adsorption-desorption isotherms of the 1-D nanostructures comprising nanorods obtained after selenization at 400 °C and subsequent oxidation at 400, 500, and 600°C.

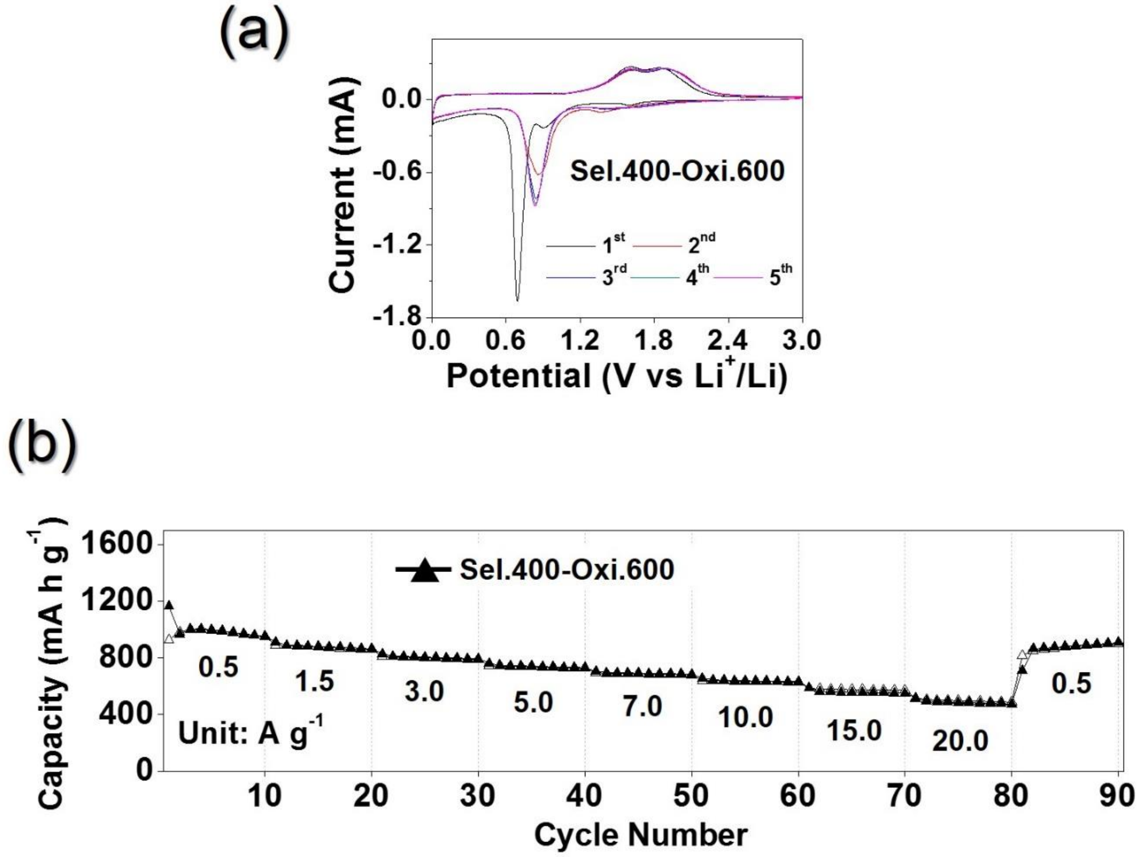

Fig. S5. (a) CV curves and (b) rate performance of the 1-D nanostructure comprising dense Fe_2O_3 nanorods (Sel.400-Oxi.600).

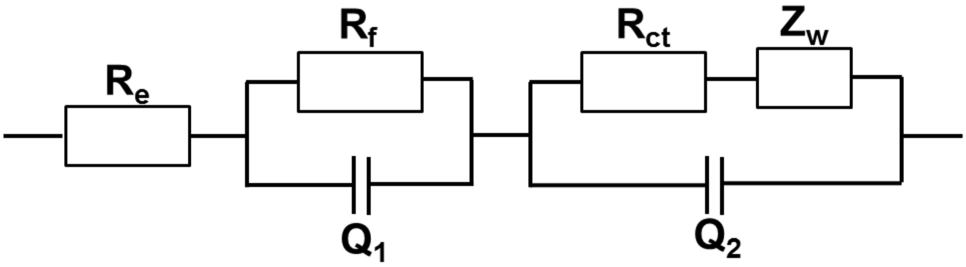

R_e : the electrolyte resistance, corresponding to the intercept of high frequency semicircle at Z_{re} axis

R_f : the SEI layer resistance corresponding to the high-frequency semicircle

Q_1 : the dielectric relaxation capacitance corresponding to the high-frequency semicircle

R_{ct}: the denote the charger transfer resistance related to the middle-frequency semicircle

Q_2 : the associated double-layer capacitance related to the middle-frequency semicircle

Z_w : the Li-ion diffusion resistance

Fig. S6. Randle-type equivalent circuit model used for AC impedance fitting.

FeSe$_2$ nanorods-C composite shows good lithium-ion storage characteristics. The discharge and charge capacities of the FeSe$_2$ nanorods-C composite were 928 and 923 mA h g^{-1}, respectively, after the 200th cycle. However, the capacities are smaller than those of 1-D nanostructure comprising porous Fe_2O_3/Se composite nanorods prepared by subsequent oxidation process.

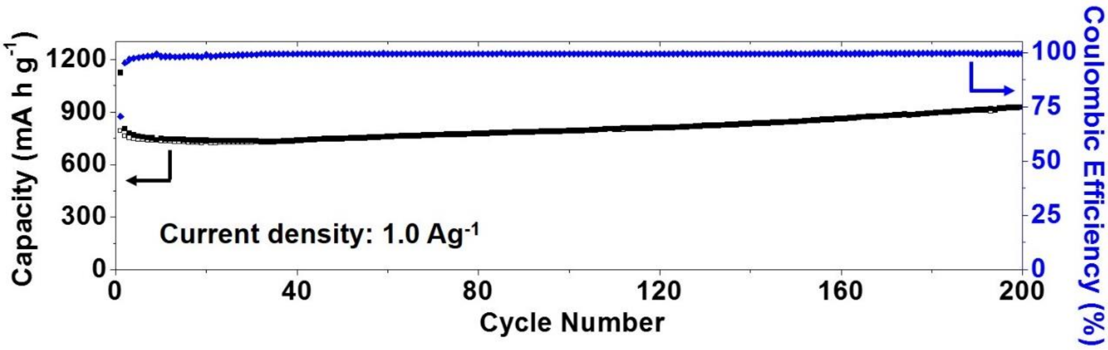

Fig. S7. Cycling performance of the FeSe$_2$ nanorods-C composite before oxidation process at a current density of 1.0 A g^{-1}.

Table S1. Electrochemical properties of the Fe oxide materials with various structures as anode materials for LIBs.

Morphology	Voltage range [V]	Current density [mA g^{-1}]	Initial Discharge Capacity [mA h g^{-1}]	Initial Coulombic Efficiency [%]	Final discharge capacity [mA h g^{-1}] and (cycle number)	Ref.
1-D nanostructure comprising porous Fe_2O_3/Se composite nanorods	0.005-3.0	1000	1458	76	1456 (400)	***This work***
Fe_2O_3 hollow sphere	0.05-3.0	200	1219	79	710 (100)	S1
Hierarchical hollow sphere composed of Fe_2O_3 nanosheets	0.01-3.0	500	1255	67	815 (200)	S2
Fe_2O_3 microbox with hierarchical shell	0.01-3.0	200	1180	71	945 (30)	S3
Fe_2O_3 hollow nanosphere	0.005-3.0	250	1435	70	490 (50)	S4
Fe_2O_3 hollow nanoparticles/ N-doped graphene aerogels	0.01-3.0	100	1586	64	1483 (100)	S5
Fe_2O_3 hollow nanobarrels	0.01-3.0	500	~1290	75	916 (100)	S6
Multi-shelled Fe_2O_3 hollow sphere	0.05-3.0	400	1360	72	861 (50)	S7
Graphene-constructed hollow sphere	0.01-3.0	100	1353	82	950 (50)	S8
Hierarchical Fe_3O_4@ polypyrrole nanocages	0.01-3.0	200	1289	75	950 (100)	S9
Hollow Fe_2O_3 sphere with carbon coating	0.01-3.0	300	1290	69	720 (140)	S10

Table S2. Electrochemical properties of the Fe related chalcogenide materials with various structures as anode materials for LIBs.

Morphology	Voltage range [V]	Current density [mA g^{-1}]	Initial discharge capacity [mA h g^{-1}]	Initial Coulombic efficiency [%]	Final discharge Capacity [mA h g^{-1}] and (cycle number)	Ref.
$FeSe_2$–C composite nanofibers	0.005-3.0	1000	1123	71	927 (200)	***This work***
Reduced graphene oxide wrapped FeS nanocomposite	0.005-3.0	100	1357	82	978 (40)	S11
FeS_2 nanowire	1.1-2.4	89	668	61	350 (50)	S12
TiO_2 modified FeS nanostructure	0.01-3.0	200	920	76	635 (100)	S13
FeS_2 microspheres wrapped by reduced graphene oxide	0.01-3.0	890	763	68	970 (300)	S14
FeS_2/C composite	1.2-2.6	44.5	784	79	495 (50)	S15
$FeSe_2$ nanoflowers	1.1-2.6	40	389	-	242 (25)	S16
Layer structured α-FeSe	1.2-2.5	40	390	90	340 (40)	S17

References

S1. B. Wang, J. S. Chen, H. B. Wu, Z. Wang, X. W. Lou, *J. Am. Chem. Soc.*, 2011, **133**, 17146-17148.

S2. J. Zhu, Z. Yin, D. Yang, T. Sun, H. Yu, H. E. Hoster, H. H. Hng, H. Zhang, Q. Yan, *Energy Environ. Sci*., 2013, **6**, 987-993.

S3. L. Zhang, H. B. Wu, S. Madhavi, H. H. Hng, X. W. Lou, *J. Am. Chem. Soc.*, 2012, **134**, 17388-17391.

S4. M. Sasidharan, N. Gunawardhana, M. Yoshio, K. Nakashima, *Ionics*, 2013, **19**, 25-31.

S5. L. Liu, X. Yang, C. Lv, A. Zhu, X., Zhu, S. Guo, C. Chen, D. Yang, *ACS Appl. Mater. Interfaces*, 2016, **8**, 7047-7053.

S6. K. S. Lee, S. Park, W. Lee, Y. S. Yoon, *ACS Appl. Mater. Interfaces*, 2016, **8**, 2027-2034.

S7. Z. Padashbarmchi, A. H. Hamidian, H. Zhang, L. Zhou, N. Khorasani, M. Kazemzad, C. Yu, *RSC Adv.*, 2015, **5**, 10304-10309.

S8. Y. Chen, J. Wang, J. Jiang, M. A. Zhou, J. Zhu, S. Han, *RSC Adv.*, 2015, **5**, 21740-21744.

S9. J. Liu, X. Xu, R. Hu, L. Yang, M. Zhu, *Adv. Energy Mater.*, 2016, **6**, 1600256.

S10. Z. Du, S. Zhang, J. Zhao, X. Wu, R. Lin, *J. Nanosci. Nanotechnol.*, 2013, **13**, 3602-3605.

S11. L. Fei, Q. Lin, B. Yuan, G. Chen, P. Xie, Y. Li, Y. Xu, S. Deng, S. Smirnov, H. Luo, *ACS Appl. Mater. Interfaces*, 2013, **5**, 5330-5335.

S12. L. Li, M. Cabán-Acevedo, S. N. Girard, S. Jin, *Nanoscale*, 2014, **6**, 2112-2118.

S13. X. Wang, Q. Xiang, B. Liu, L. Wang, T. Luo, D. Chen, G. Shen, *Sci. Rep.*, 2013, **3**, 2007-2014.

S14. H. Xue, Y. W. Denis, J. Qing, X. Yang, J. Xu, Z. Li, M. Sun, W. Kang, Y. Tang, C. S. Lee, *J. Mater. Chem. A*, 2015, **3**, 7945-7949.

S15. D. Zhang, Y. J. Mai, J. Y. Xiang, X. H. Xia, Y. Q. Qiao, J. P. Tu, *J. Power Sources*, 2012, **217**, 229-235.

S16. L. Q. Mai, Y. Gao, J. G. Guan, B. Hu, L. Xu, W. Jin, *Int. J. Electrochem. Sci*, 2009, **4**, 755-761.

S17. D. Wei, J. Liang, Y. Zhu, L. Hu, K. Zhang, J. Zhang, Z. Yuan, Y. Qian, Y. *Electrochem. Commun.*, 2014, **38**, 124-127.